

# The infrared conductivity of $\text{Na}_x\text{CoO}_2$ : evidence of gapped states.

J. Hwang<sup>1</sup>, J. Yang<sup>1</sup>, T. Timusk<sup>1,2</sup> and F.C. Chou<sup>3</sup>

<sup>1</sup>*Department of Physics and Astronomy,*

*McMaster University, Hamilton ON L8S 4M1, Canada*

<sup>2</sup>*The Canadian Institute of Advanced Research, Canada*

<sup>3</sup>*Center for Materials Science and Engineering,*

*MIT, Cambridge, MA 02139, USA\**

## Abstract

We present infrared ab-plane conductivity data for the layered cobaltate  $\text{Na}_x\text{CoO}_2$  at three different doping levels ( $x = 0.25, 0.50$ , and  $0.75$ ). The Drude weight increases monotonically with hole doping,  $1 - x$ . At the lowest hole doping level  $x=0.75$  the system resembles the normal state of underdoped cuprate superconductors with a scattering rate that varies linearly with frequency and temperature and there is an onset of scattering by a bosonic mode at  $600 \text{ cm}^{-1}$ . Two higher hole doped samples ( $x = 0.50$  and  $0.25$ ) show two different-size gaps ( $110 \text{ cm}^{-1}$  and  $200 \text{ cm}^{-1}$ , respectively) in the optical conductivities at low temperatures and become insulators. The spectral weights lost in the gap region of  $0.50$  and  $0.25$  samples are shifted to prominent peaks at  $200 \text{ cm}^{-1}$  and  $800 \text{ cm}^{-1}$ , respectively. We propose that the two gapped states of the two higher hole doped samples ( $x=0.50$  and  $0.25$ ) are pinned charge ordered states.

PACS numbers: 74.25.Kc, 74.25.Gz

The recently discovered cobalt oxide superconductor  $\text{Na}_x\text{CoO}_2 \cdot y\text{H}_2\text{O}$ , with  $1/4 < x < 1/3$  and  $y=1.4^{1,2,3,4}$ , resembles in many ways that other famous family of oxide superconductors, the cuprates. The cobaltate structure is based on two-dimensional planes, weakly coupled in the third direction, the  $c$ -axis. The Co ions are on a triangular lattice and calculations based on the  $t$ - $J$  model suggest that the material may give rise to novel quantum states<sup>5,6</sup>. The  $\text{Na}_x\text{CoO}_2$  material with  $x = 0.75$  appears to be metallic with a Curie-Weiss susceptibility<sup>7,8</sup>. With increased hole doping,  $1-x$ , (smaller  $x$ ) the  $\text{Na}_x\text{CoO}_2$  material shows a different metallic state with a temperature independent paramagnetic susceptibility<sup>8</sup>. Separating the two metallic regions is an insulating state at  $x = 0.50$ <sup>8</sup>. In this state a superstructure develops in the Na plane that separates the CoO planes and it has been suggested that the insulating state is induced by this superstructure<sup>8</sup>. Other charge ordered states that compete with superconductivity have been proposed at higher hole doping levels than 0.50<sup>9,10</sup>. Here we present optical data that show evidence of *two* gapped insulating states, one at  $x = 0.50$  and a new one at a higher hole doping level close to  $x = 0.25$ .

We use optical spectroscopy to investigate the low-lying states of the normal state of  $\text{Na}_x\text{CoO}_2$  at three different doping levels ( $x = 0.75$ ,  $0.50$ , and  $0.25$ ) at various temperatures. Previous optical work has been confined to the  $\text{Na}_x\text{CoO}_2$  materials with low hole doping levels,  $x$  above  $0.50$  ( $x = 0.57$ ,  $0.70$ , and  $0.82$ )<sup>11,12,13,14</sup>. A metallic Drude-like absorption is found with anomalous linear frequency dependence of the scattering rate. The infrared reflectance resembles that of the cuprates with the reflectance decreasing linearly with frequency over a broad region extending to nearly  $0.75$  eV. As the temperature is lowered below room temperature, a knee develops in the reflectance at  $600 \text{ cm}^{-1}$ , characteristic of the interaction of the charge carriers with a bosonic mode<sup>15,16</sup>. We complement this work by extending it to higher hole doping levels, examining electro-chemically doped samples with  $x = 0.25$  and  $0.50$ . We also studied an as-grown sample with  $x = 0.75$ .

The preparation of the samples has been described previously<sup>3</sup>. The parent  $\text{Na}_x\text{CoO}_2$  single crystals are grown by the floating zone method. Na atoms which reside between the tilted octahedral cobalt oxide layers were deintercalated in a electrochemical cell. The Na concentration was determined by electron probe microanalysis (EPMA) and we estimate the uncertainty in  $x$  to be  $\pm 0.08$ . The hole doping of the cobalt oxide layers is thought generally to be proportional to  $1 - x$  but it should be noted that there have been reports of other sources carriers such as oxygen deficiency<sup>17,18</sup> or interlayer oxonium ion<sup>19,20,21</sup> making

the Na concentration a less reliable indicator of the in-plane doping level. As we will show below a more direct measure of doping is the Drude spectral weight which we will use as our main guide in determining the planar hole concentration.

The optical experiments were performed on freshly cleaved ab-plane surface of  $2 \times 2 \text{ mm}^2$  crystals in a  $^4\text{He}$  flow cryostat. The ab-plane reflectance was measured between 50 and 40 000  $\text{cm}^{-1}$  using an *in situ* gold evaporation method<sup>22</sup>. We estimate the absolute accuracy of the reflectance to be better than 0.5 %. For Kramers-Kronig (KK) analysis we used the dc resistivity<sup>23</sup> to extend the data at low frequency. At high frequencies we used a data of Caimi *et al.*<sup>14</sup> between 40 000 and 100 000  $\text{cm}^{-1}$  and extrapolations assuming a free carrier response beyond 100 000  $\text{cm}^{-1}$ .

Fig. 1a shows the overall reflectance at each of the three doping levels at room temperature. The reflectance has a characteristic linear variation with frequency with the slope of the curve decreasing as the materials become more metallic at the higher hole doping levels. This is similar to what happens in the cuprates where the reflectance slope can be used as an internal standard of the doping level<sup>24</sup>. Using this criterion, we can see that three different samples show reflectances that follow the Na doping levels monotonically.

Fig. 1b shows the frequency dependent conductivity at room temperature at the three doping levels obtained by KK analysis of the reflectance. The dc resistivity is marked on the ordinate axis. We see a low frequency Drude-like band but with a high frequency tail that could be interpreted as an additional absorption band in the mid-infrared. Following Wang *et al.*<sup>12</sup> we will call this the  $\gamma$  band. A second prominent band, the  $\beta$  band can be seen at 15 000  $\text{cm}^{-1}$  as well as a third one  $\alpha$  at 26 000  $\text{cm}^{-1}$ . We see that as the hole doping level increases there is a strong growth of both the  $\gamma$  and the  $\beta$  band intensities as well as the Drude weight.

The monotonic variation of Drude weight with doping is illustrated in Fig. 1c where we show the partial spectral weight, obtained by integrating the optical conductivity,  $N_{eff}(\omega_c) = 2mV_{Co}/(\pi e^2) \int_0^{\omega_c} \sigma_1(\omega) d\omega$ , where  $m$  is the mass of an electron,  $V_{Co}$  is the volume per Co atom,  $e$  is the charge of an electron, and  $\sigma_1$  is the optical conductivity. The flat region between 5000 to 8000  $\text{cm}^{-1}$  separates the Drude weight from the  $\beta$  band weight. The figure shows that the Drude weight grows monotonically with hole doping and that the Drude absorption becomes sharper and hence better defined as the hole doping level increases. Viewed in this high frequency region and at room temperature, the system becomes more metallic with

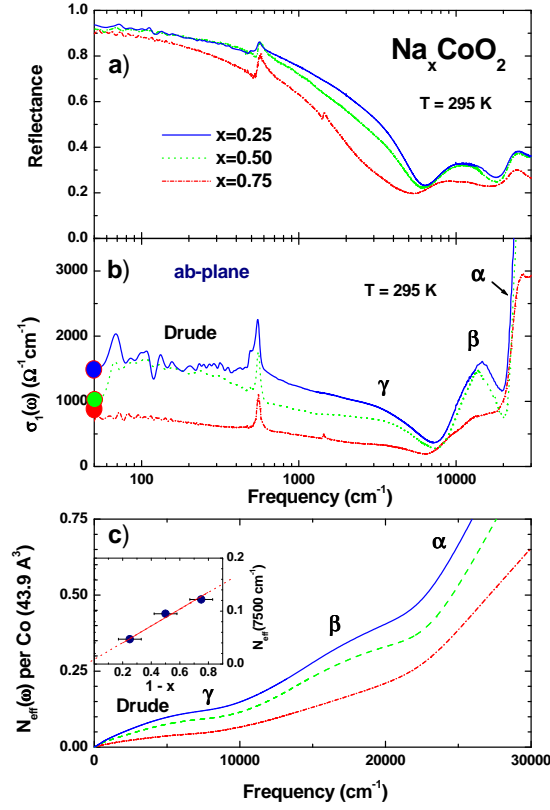


FIG. 1: a) The ab-plane reflectance of  $\text{Na}_x\text{CoO}_2$  at three doping levels, at room temperature. b) The ab-plane optical conductivity of  $\text{Na}_x\text{CoO}_2$  at the three doping levels at room temperature. We see a broad Drude-like band at low frequency in all samples characteristic of an overall metallic conductivity. At higher frequency there are bands denoted  $\gamma$  and  $\beta$ . There is a rapid growth of spectral weight of the low lying bands  $\gamma$  and  $\beta$  with doping. c) Partial sum rule for the three doping levels. The Drude weight grows monotonically with hole doping, shown by the flat region between  $5000\text{ cm}^{-1}$  and  $8000\text{ cm}^{-1}$ . The inset shows the spectral weight integrated up to  $7500\text{ cm}^{-1}$  with error bars  $\pm 3\%$  as a function of hole doping with error bars  $\pm 0.08$ .

hole doping. However, as we will see, at low frequency and low temperature the two more highly hole-doped samples ( $x = 0.50$  and  $0.25$ ) are actually insulators. It is interesting to note that there is no transfer of spectral weight from the  $\alpha, \beta$  and  $\gamma$  bands to the Drude component as the hole doping level is increased as seen in the  $\text{La}_{2-x}\text{Sr}_x\text{CuO}_4$  cuprates<sup>25</sup>.

The optical properties of the  $0.75$  sample resemble those of the underdoped cuprates superconductors. Fig. 2a shows the optical conductivity of the  $x = 0.75$  sample at a series of temperatures, from  $295\text{ K}$  to  $28\text{ K}$ . At room temperature we see a broad Drude-like band

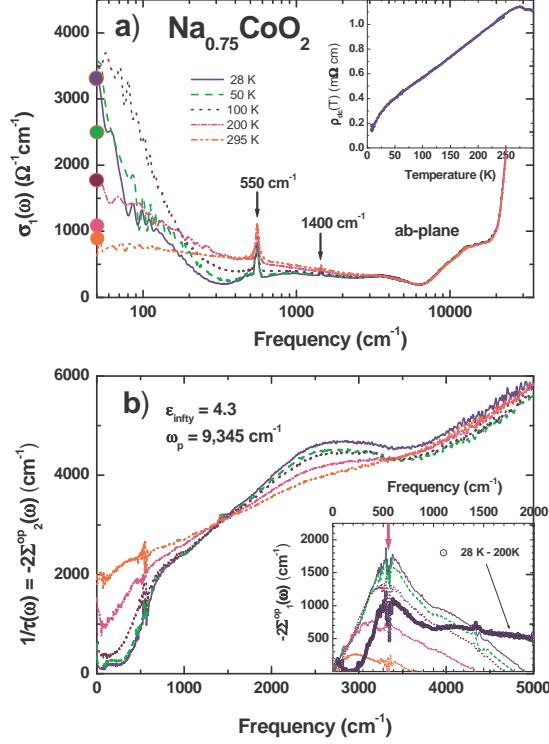


FIG. 2: a) The temperature dependence of the ab-plane optical conductivity of the  $x = 0.75$  sample and dc resistivity in the inset. b) The scattering rate  $1/\tau$ . Here we subtracted the phonons at 550 and 1400  $\text{cm}^{-1}$  to see the bosonic mode better<sup>16</sup>. The inset shows the imaginary part of the optical scattering rate or the real part of the optical self-energy. The contribution of the bosonic mode can be separated from the broad background scattering.

which splits at low temperature into two components, a zero-frequency-centered coherent band and a broad band at 1000  $\text{cm}^{-1}$  separated by a slight gap-like depression in the 300  $\text{cm}^{-1}$  region. We also observe two phonons at 550 and 1400  $\text{cm}^{-1}$ . Drawing on our experience in the cuprates, we can better illustrate the physics involved here by plotting the real and imaginary parts of the scattering rate (or the optical self-energy) using the extended Drude model<sup>16,26</sup>, shown in Fig. 2b and the inset. Here  $\sigma_1(\omega) = \omega_p^2/[4\pi(\omega - 2\Sigma^{op}(\omega))]$ , where  $\omega_p$  is the plasma frequency and  $\Sigma^{op}(\omega) = \Sigma_1^{op}(\omega) + i\Sigma_2^{op}(\omega)$  is the complex optical self-energy. Two phonons at 550 and 1400  $\text{cm}^{-1}$  have been removed to allow us to see the bosonic mode better. Note that the scattering rate is always greater than the frequency and there are no coherent quasiparticles except perhaps at the lowest temperatures. We also see that the low-frequency scattering is dominated by a bosonic mode with an onset frequency of scattering of

the order of  $600 \text{ cm}^{-1}$ . The contribution of the mode weakens as the temperature increases and the scattering is dominated by a strong linear-in-frequency process, very much like that in the cuprates<sup>16</sup>. In this picture of a linear background and a mode, the dc resistivity shows a positive curvature in the temperature region where the mode becomes activated<sup>27</sup>. The mode and the background can be separated by plotting the imaginary part of the scattering rate or the real part of the optical self-energy<sup>16</sup>, shown in the inset, along with a difference spectrum where we have subtracted the 200 K spectrum from the 28 K spectrum. The mode can be seen as a sharp peak around  $600 \text{ cm}^{-1}$  superimposed on the broad background. This line shape is very similar to what is seen in the underdoped cuprates<sup>16</sup>. At low temperatures the scattering rate spectrum develops a broad peak at  $3000 \text{ cm}^{-1}$ . This is reminiscent of the mid-infrared absorption seen in the single layer cuprates at low doping levels<sup>25</sup>.

Fig. 3a shows the frequency dependent conductivity of the  $x = 0.50$  sample at various temperatures. We show the dc conductivity on the zero frequency axis as well. The dc resistivity shows insulating behavior with the 53 K and 88 K anomalies (see inset of Fig. 3a). We notice that there is an overall agreement between the lowest measured infrared conductivity and the dc conductivity. This is evidence of two important facts. First, the samples are reasonably homogeneous without any channels and inhomogeneities that might short circuit the current. Second, there are no low-lying collective modes in the spectral region between zero frequency and  $50 \text{ cm}^{-1}$ , our lowest measured frequency. This is not always the case in strongly correlated systems. In the one-dimensional organic conductors there is a large discrepancy between the highly metallic dc conductivity and nearly insulating gap-like behavior in the infrared, a signature of sliding charge-density wave(CDW) transport<sup>28</sup>. There is no evidence for such effects in our samples of  $\text{Na}_x\text{CoO}_2$ , although it should be noted that there is about a factor of two discrepancy between the dc values and the peak that develops around  $100 \text{ cm}^{-1}$ . This is similar to what is seen in the cuprates at low frequency and has been attributed to localization effects<sup>29</sup>. There is evidence of similar localization effects in the  $x = 0.75$  sample where there is also a discrepancy at low temperature between the dc and the lowest far infrared measurement and the dc conductivity. In all cases the dc value is *lower* suggesting localization, whereas in the CDW systems with sliding waves, the dc value is *higher* by a substantial factor.

This system shows very interesting temperature dependent properties at low frequencies as expected from the temperature dependence of the dc resistivity. There is a sharpening of

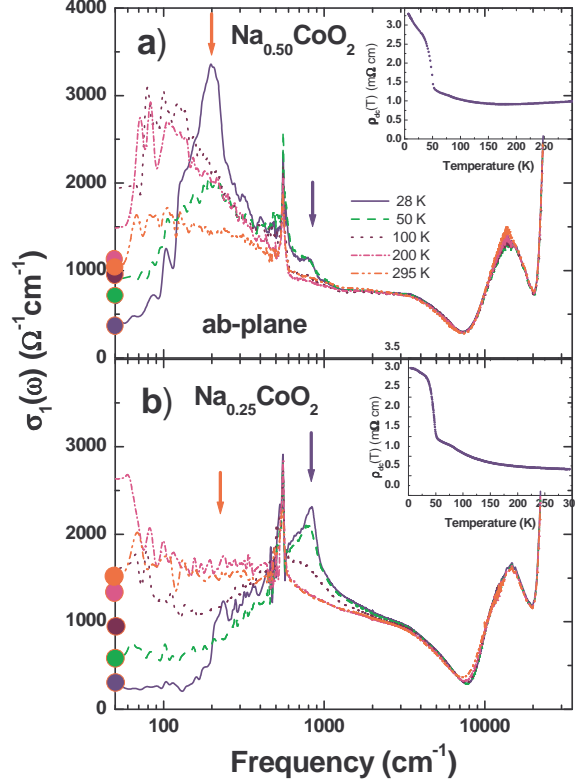


FIG. 3: a) Temperature dependence of the optical ab-plane conductivity of the  $x = 0.50$  sample and its dc resistivity in the inset. b) The optical conductivity of the  $x = 0.25$  sample and its dc resistivity in the inset. The symbols on the vertical axis denote the dc conductivity of the samples. We see that when the temperature is lowered both samples become more insulating due to the formation of a gap in the spectrum. The spectral weight removed from the gap is transferred to the peaks at higher frequencies delineated by arrows.

the free carrier peak as the temperature is lowered from 295 to 200 K. Between 200 and 100 K the spectra do not change much. Below 100 K a gap develops rapidly and is accompanied by a sharp peak at  $200\text{ cm}^{-1}$ . At our lowest temperature 28 K the gap seems fully developed with a width  $110\text{ cm}^{-1}$ . In agreement with this overall energy scale, the spectral weight lost in the gap region is recovered by  $600\text{ cm}^{-1}$ . These changes in the optical properties are clear evidence of a low temperature pinned density wave phase with a resonance frequency  $200\text{ cm}^{-1}$ .

Fig. 3b shows the conductivity of the most highly hole doped sample with  $x = 0.25$  at different temperatures. Again, there is reasonable agreement between the dc and infrared magnitudes of the conductivity suggesting insulating behavior and the absence of sliding

density waves. The dc resistivity also shows insulating behavior with 53 K and 88 K anomalies (see inset of Fig. 3b). Similar 52 K anomaly has been observed in a highly hole doped and fully hydrated sodium cobaltate,  $\text{Na}_{0.30}\text{CoO}_2 \cdot 1.4\text{H}_2\text{O}^4$ . The origin of the anomaly in the dc resistivity of high hole doped systems is not clear yet.

The gap-like depression of conductivity below  $200\text{ cm}^{-1}$  in the  $x = 0.25$  sample starts to develop between 200 and 100 K and is nearly fully formed at 28 K, our lowest measured temperature. Like the pseudogap seen in c-axis transport in the cuprates, the gap here does not close at temperature but has a constant width and fills in as the temperature is raised. There is a notable sharp peak at  $800\text{ cm}^{-1}$  that grows in parallel with the gap. It starts below 200 K and has its most rapid rate of increase between 100 K and 50 K. There is a transfer of spectral weight from the gap to the peak, and by  $1000\text{ cm}^{-1}$ , nearly all the spectral weight lost in the gap region has been recovered. The size and the onset temperature of the gap, the center frequency of the sharp peak, and the spectral weight recovering frequency in the  $x = 0.25$  sample are higher than the corresponding ones in the 0.50 sample. These factors strongly suggest that there is a distinct and separate pinned CDW insulating phase in the 0.25 system.

It is interesting to note that in the 0.50 sample there is a weak remnant of the  $800\text{ cm}^{-1}$  mode suggesting that the sample may have an admixture of the 0.25 phase, about 15 % based on the spectral weight of the peaks. Similarly, it is possible that the feature  $230\text{ cm}^{-1}$  seen in the 0.25 sample may be related to a minority phase of the 0.50 peak at  $200\text{ cm}^{-1}$ , about less than 2 % based on the spectral weight of the peaks. The peaks are denoted by arrows in the figures.

The only transverse optic phonon that can be seen in the spectra is a sharp peak at  $550\text{ cm}^{-1}$ . Its spectral weight ( $\omega_p = 870\text{ cm}^{-1}$ ) is consistent with what is expected for a phonon that involves oxygen motion. In the  $x = 0.75$  crystal there is an additional phonon mode at  $1400\text{ cm}^{-1}$  that we attribute to a small amount of carbonate, one of the starting materials of the synthesis process. The  $550\text{ cm}^{-1}$  mode in the  $x = 0.50$  sample appears to split between 100 K and 50 K. The  $550\text{ cm}^{-1}$  mode in 0.75 sample does not show any splitting as temperature is lowered. The  $550\text{ cm}^{-1}$  mode acquires a slight Fano shape below 100 K at the highest hole doping levels. We do not observe, in any of our samples, the dramatically enhanced spectral weight of phase phonons associated with CDW order seen in the organic charge transfer salts<sup>30</sup>.



There is an alternate explanation of our results on the two insulating samples in terms of two different pinning sites for the charge density waves with the stronger pinning potential dominating at the higher doping level. However, to explain the fact that we have two insulating samples with Drude weight that differs by 20 % we have to assume that the insulating region in the phase diagram at  $x = 0.5$  is quite wide. Another possibility that could account for the extra spectral weight in the 0.25 sample is a two-phase system with metallic drops present in the insulating host. This can be ruled out since such drops would not add to the Drude weight but give a high frequency band at  $\omega_p/\sqrt{3}$ .

In summary the optical conductivity of  $\text{Na}_x\text{CoO}_2$  has many common elements with the cuprate high temperature superconductors but there are also striking differences. The free carrier absorption is dominated by a continuum of scattering processes that extend to nearly 0.75 eV in energy. For the 0.75 sample, as the temperature is lowered, a bosonic mode appears, very much like the mode that has been attributed to the magnetic resonance in the cuprates<sup>15,16</sup>. The mode even has a frequency close to that of the cuprates.

The two samples with the higher hole doping levels ( $x = 0.50$  and  $0.25$ ) become insulators at low frequency and low temperature as results of the development of two different size gaps and pinning resonance peaks that are quite a bit higher than similar features seen in the cuprates<sup>31,32,33</sup>. There are localization effects in the cuprates, but these are hard to observe because of the appearance of the superconducting state<sup>34</sup>. In contrast, in  $\text{Na}_x\text{CoO}_2$  the charge ordering potentials are much stronger giving rise to clear gaps in 0.50 and 0.25 materials as well as absorption peaks at quite high frequencies. These may be processes that compete with superconductivity and may be the cause of the absence of superconductivity of  $\text{Na}_x\text{CoO}_2$  or the relatively low superconducting transition temperatures of  $\text{Na}_x\text{CoO}_2$  system with additional  $\text{H}_2\text{O}$  layers. On the positive side, it seems that the basic attractive force in the two systems is very similar suggesting that if the competing charge order can be suppressed by the manipulation of the Na lattice a higher superconducting  $T_c$  may be possible in this system.

## Acknowledgments

We thank Patrick Lee and Takashi Imai for encouragement and helpful discussions. The crystal growth at MIT was primarily supported by the MSEC program of the National

- \* Electronic address: timusk@mcmaster.ca
- <sup>1</sup> K. Takada, H. Sakurai, E. Takayama-Muromachi, F. Izumi, R. A. Dilanian, and T. Sasaki, *Nature* **422**, 453 (2003).
- <sup>2</sup> R. E. Schaak, T. Klimczuk, M. L. Foo, and R. J. Cava, *Nature* **424**, 527 (2003).
- <sup>3</sup> F. C. Chou, J. H. Cho, P. A. Lee, E. T. Abel, K. Matan, and Y. S. Lee, *Phys. Rev. Lett.* **92**, 157004 (2004).
- <sup>4</sup> R. Jin, B. C. Sales, P. Khalifah, and D. Mandrus, *Phys. Rev. Lett.* **91**, 217001 (2003).
- <sup>5</sup> G. Baskaran, *Phys. Rev. Lett.* **91**, 097003 (2003).
- <sup>6</sup> Q.H. Wang, D.H. Lee, and P.A. Lee, *Phys. Rev. B* **69**, 092504 (2004).
- <sup>7</sup> R. Ray, A. Ghoshray, K. Ghoshray, and S. Nakamura, *Phys. Rev. B* **59**, 9454 (1999).
- <sup>8</sup> M. L. Foo, Y. Wang, S. Watauchi, H. W. Zandbergen, T. He, R. J. Cava, and N. P. Ong, *Phys. Rev. Lett.* **92**, 247001 (2004).
- <sup>9</sup> G. Baskaran, cond-mat/0306569 (2004).
- <sup>10</sup> W. Koshibae and S. Maekawa, *Phys. Rev. Lett.* **91**, 257003 (2003).
- <sup>11</sup> S. Lupi, M. Ortolani, and P. Calvani, *Phys. Rev. B* **69**, 180506(R) (2004).
- <sup>12</sup> N. L. Wang, P. Zheng, D. Wu, Y. C. Ma, T. Xiang, R. Y. Jin, and D. Mandrus, *Phys. Rev. Lett.* **93**, 237007 (2004).
- <sup>13</sup> C. Bernhard, A. V. Boris, N. N. Kovaleva, G. Khaliullin, A.V. Pimenov, L. Yu, D. P. Chen, C. T. Lin, and B. Keimer, *Phys. Rev. Lett.* **93**, 167003 (2004).
- <sup>14</sup> G. Caimi, L. Degiorgi, H. Berger, N. Barisic, L. Forro, and F. Bussy, cond-mat/0404400 (2004).
- <sup>15</sup> J.P. Carbotte, E. Schachinger, and D.N. Basov, *Nature* **401**, 354 (1999).
- <sup>16</sup> J. Hwang, T. Timusk, and G. D. Gu, *Nature* **427**, 714 (2004).
- <sup>17</sup> F.C. Chou, E.T. Abel, J.H. Cho, and Y.S. Lee, cond-mat/0405158 (2004).
- <sup>18</sup> M. Banobre-Lopez, F. Rivadulla, R. Caudillo, M.A. Lopez-Quintela, J. Rivas, and J.B. Goode-nough, cond-mat/0409606 (2004).
- <sup>19</sup> K. Takada, K. Fukuda, M. Osada, I. Nakai, F. Izumi, R.A. Dilanian, K. Kato, M. Takata, H. Sakurai, E. Takayama-Muromach, and T. Sasaki, *J of Material Chemistry* **14**, 1448 (2004).
- <sup>20</sup> C.J. Milne, D.N. Argyriou, A. Chemseddine, N. Aliouane, J. Veira, S. Landsgesell, and D.

- Alber, Phys. Rev. Lett. **93**, 247007 (2004).
- <sup>21</sup> X.H. Chen, C.H. wang, H.T. Zhang, X.X. Lu, and G. Wu, cond-mat/0501181 (2004).
- <sup>22</sup> C. C. Homes, M. A. Reedyk, D. A. Crandles, and T. Timusk, Appl. Opt. **32**, 2976 (1993).
- <sup>23</sup> The dc resistivity of the crystals used in the optical data were measured with a van der Pauw method for each doping level, see also Khaykovich *et al.*, unpublished.
- <sup>24</sup> J. Hwang, T. Timusk, A.V. Puchkov, N. L. Wang, G. D. Gu, C.C. Homes, J.J. Tu, and H. Eisaki, Phys. Rev. B **69**, 094520 (2004).
- <sup>25</sup> S. Uchida, T. Ido, H. Takagi, T. Arima, Y. Tokura, and S. Tajima, Phys. Rev B **43**, 7942 (1991).
- <sup>26</sup> A.V. Puchkov, D.N. Basov, and T. Timusk, J. Physics, Condensed Matter, **8**, 10049 (1996).
- <sup>27</sup> Y. Ando, S. Komiya, K. Segawa, S. Ono, and Y. Kurita, Phys. Rev. Lett. **93**, 267001 (2004).
- <sup>28</sup> H. K. Ng, T. Timusk, and K. Bechgaard, Phys. Rev. B **30**, 5842 (1984).
- <sup>29</sup> D.N. Basov, B.Dabrowski, and T. Timusk, Phys. Rev. Letters **81**, 2132, (1998).
- <sup>30</sup> M. J. Rice, Phys. Rev. Lett. **37**, 36 (1976).
- <sup>31</sup> T. Timusk, D.N. Basov, C.C. Homes, A.V. Puchkov, and M. Reedyk, J. of Superconductivity, **8**, 437 (1995).
- <sup>32</sup> M. Dumm, D. N. Basov, S. Komiya, Y. Abe, and Y. Ando, Phys. Rev. Lett. **88**, 147003 (2002).
- <sup>33</sup> L. Benfatto and C.M. Smith, Phys. Rev. B **68**, 184513 (2003).
- <sup>34</sup> G. S. Boebinger, Yoichi Ando, A. Passner, T. Kimura, M. Okuya, J. Shimoyama, K. Kishio, K. Tamasaku, N. Ichikawa, and S. Uchida, Phys. Rev. Lett. **77**, 5417 (1996).